LETTER TO THE EDITOR

The spectroscopic evolution of the recurrent nova T Pyxidis during its 2011 outburst[⋆]

I. The optically thick phase and the origin of moving lines in novae

S. N. Shore[1], T. Augusteijn[2], A. Ederoclite[3,4], and H. Uthas[5]

[1] Dipartimento di Fisica "Enrico Fermi", Università di Pisa, and INFN – Sezione Pisa, largo B. Pontecorvo 3, 56127 Pisa, Italy
e-mail: shore@df.unipi.it
[2] Nordic Optical Telescope, Apartado 474, 38700 Santa Cruz de La Palma, Santa Cruz de Tenerife, Spain
e-mail: tau@not.iac.es
[3] Instituto de Astrofísica de Canarias, 38200 La Laguna, Tenerife, Spain
e-mail: ale@iac.es
[4] Departamento de Astrofísica, Universidad de La Laguna, 38206 La Laguna, Tenerife, Spain
[5] Department of Astronomy, Columbia University, 550 W 120th Street, New York, NY 10027, USA
e-mail: helena@astro.columbia.edu

ABSTRACT

Aims. We aim to derive the physical properties of the recurrent nova T Pyx and the structure of the ejecta during the early stages of expansion of the 2011 outburst.
Methods. The nova was observed with high resolution spectroscopy ($R \approx 65\,000$), from one day after discovery of the outburst and until the last visibility of the star at the end of May 2011. The interstellar absorption lines of Na I, Ca II, CH, CH$^+$, and archival H I 21 cm emission line observations were used to determine a kinematical distance. Interstellar diffuse absorption features have been used to determine the extinction independent of previous assumptions. Sample Fe-peak line profiles show the optical depth and radial velocity evolution of the discrete components.
Results. We propose a distance to T Pyx ≥ 4.5 kpc, with a strict lower limit of 3.5 kpc (the previously accepted distance). We derive an extinction, $E(B - V) \approx 0.5 \pm 0.1$, that is higher than previous estimates. The first observation, Apr. 15, displayed He I, He II, C III, and N III emission lines and a maximum velocity derived from the P Cyg profiles of the Balmer and He I lines of ≈ 2500 km s^{-1} that is characteristic of the fireball stage. These ions were undetectable in the second spectrum, Apr. 23, and we use the recombination time to estimate the mass of the ejecta, $10^{-5} f\ M_\odot$ for a filling factor f. Numerous absorption-line systems were detected in the Balmer, Fe-peak, Ca II, and Na I lines, mirrored in broader emission-line components, that showed an "accelerated" displacement in velocity. We also show that the time sequence of these absorptions, which are common to all lines and arise only in the ejecta, can be described by a recombination front moving outward in the expanding gas without either a stellar wind or circumstellar collisions. By the end of May, the ejecta were showing signs of turning optically thin in the ultraviolet.

Key words. novae – cataclysmic variables – stars: individual: T Pyx

1. Introduction

Classical novae (CNe) are thought to be the result of the thermonuclear runaway on the surface of a white dwarf that is accreting mass from a Roche-lobe filling companion (see the recent compilation by Bode & Evans 2008). Since the system survives the eruption, a CN is a repeating phenomenon, although the recurrence time (i.e. the time between two consecutive explosions) is $>10^3$ yr. Recurrent novae (RNe) display repeat outbursts with a much higher frequency, on intervals of <100 yr, The system T Pyx bears greater resemblence to the CNe in having a Roche-lobe filling companion and orbital period shorter than one day. It was discovered in 1890 and underwent outbursts at nearly regular intervals in 1902, 1920, 1944, and 1967. It then went into a dormant state for unknown reasons. The wait ended when the sixth outburst was discovered on the 2011 Apr. 14.29 (JD 2 455 665.79, IAUC 9205). The orbital period was determined by Uthas et al. (2010) to be 1.83 h by

spectroscopy during the hiatus interval. They derived a WD mass of $M_{\rm WD} = 0.7 \pm 0.2\ M_\odot$. This depends on the assumed mass for the companion, $M_{\rm comp}$ and is, in fact, a lower limit since their radial velocity curve only yields a robust estimate for the mass ratio, $M_{\rm WD}/M_{\rm comp} \approx 0.2$. In contrast, a model for RNe need to include a high-mass WD to explain such high recurrence rates (see Starrfield et al. 2008; Starrfield & Iliadis 2008).

2. Observational data

Our data set consists of spectra taken between 2011 Apr. 15 and 2011 May 30 with the 2.6 m Nordic Optical Telescope (NOT) fiber-optic echelle spectrograph (FIES, program P40-403) with a dispersion of 0.023 Å px^{-1} in high-resolution mode, covering the spectral interval from 3635 to 7364 Å and 0.035 Å px^{-1} in medium-resolution mode, covering the spectral interval from 3680 to 7300 Å (see Table 1). Exposures ranged from 60 s to 900 s. The sequence was not absolutely calibrated. All NOT spectra were reduced using IRAF, FIESTools, and IDL[1].

⋆ Appendices are available in electronic form at
http://www.aanda.org

[1] IRAF is distributed by the National Optical Astronomy Observatories, which are operated by the Association of Universities

Table 1. Journal of NOT observations.

Date (2011)	Time (UT)	JD 2 400 000+
Apr. 15	22:07	55 667.42
Apr. 23	22:51	55 675.46
May 6	20:56	55 688.38
May 8	20:55	55 690.37
May 15	21:04	55 697.38
May 21	20:47	55 703.37
May 30	21:00	55 712.38

Table 2. Heliocentric interstellar line velocities.

Identification	λ (Å)	abs/em	$v_{\rm rad}$ km s^{-1}
Ca II K	3933.66	abs	34.5, 42.3
CH$^+$	4232.54	abs	38.4
CH	4300.31	abs	49.5
Na I D1	5889.95	abs	30.7, 40.8
Na I D2	5895.92	abs	30.4, 42.5
H I	21 cm	em	11.4, 21.9, 34.8, 81.1

3. Distance and extinction estimates

The distance and extinction to T Pyx are the parameters with the greatest uncertainty. Selvelli et al. (2008) and Schaefer (2010) provide the most recent compilations of the estimates for T Pyx, giving a distance of 3.5±1 kpc and $E(B-V) = 0.25\pm0.02$ and, for the purposes of this Letter we refer the reader to Tables 26 and 29 of Schaefer (2010) for details. Although some spectroscopy during the extended minimum was included in these previous studies, with inconclusive results, almost all estimates of both distance and reddening were based on photometry. We attempted to obtain limits on both spectroscopically. The NOT spectra contain a number of atomic and molecular absorption lines, all of which are resolved into multiple components or display asymmetric profiles in a manner that indicates more than one contributor. These are listed in Table 2 and displayed in Fig. 1. Neutral hydrogen 21 cm line profiles are available for this Galactic position ($l_{\rm II} = 257.2$, $b_{\rm II} = +9.6$) from the LAB survey (Kalberla et al. 2005) with a broad component extending from $+32$ to $+52$ km s^{-1} that spans the radial velocity interval of the atomic and molecular absorption lines. Using the Galactic rotation curve for the third quadrant (Brand & Blitz 1993) we find a *minimum* distance consistent with previous estimates, 4.0 kpc, for $\Theta_0 = 220$ km s^{-1} based on the radial velocity $v_{\rm rad}$ of the interstellar CH 4300 Å line. The center of mass velocity of the binary is still uncertain and may be variable (Uthas et al. 2010) but there may be another way of obtaining it. In the JD 55 712 spectrum, the emission lines (e.g., Fe II RMT 42, H Balmer) show two nearly symmetric emission peaks, and the same holds for the weak emergent [O I] 5577, 6300 Å emission lines with a separation of about 700 km s^{-1} and mean velocity of $+60 \pm 3$ km s^{-1} [2]. If real, this corresponds to a distance of ≈5 kpc. There are no independent interstellar measurements toward nearby OB stars in the archives. We thus conclude that the distance to T Pyx is >4 and ≤5 kpc.

[2]   In their orbital solution of T Pyx using the He II 4686 Å emission line during quiescence, Uthas et al. (2010) were unable to derive a definitive systematic velocity for the nova but all of their solutions were at a velocity lower than $+20$ km s^{-1}. We suggest that there may be a residual uncertainty caused by the profile of the He II line and/or shell emission that compromises the center-of-mass velocity but not the amplitude of the variations, 17.9 ± 1.6 km s^{-1}.
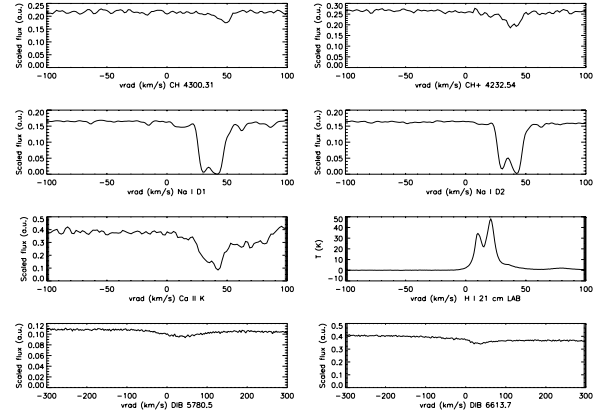
Fig. 1. Interstellar absorption lines from the spectrum taken on JD 55 697. The radial velocities are heliocentric (conversion for the H I 21 cm LAB spectrum, using 220 km s^{-1} for the LSR) (see text for discussion). Note the change in velocity scale for the DIBs in the lowest two panels.

Table 3. Diffuse interstellar bands.

| λ (Å)	EW (mÅ)	λ	EW	λ	EW
5780	280	6204	104	6613	49
5799	63	6283	284	6623	62
6196	30	6379	28	6532	22
6203	65:	5632	22	7224	50
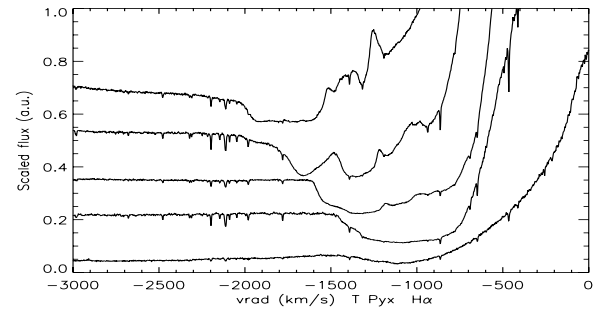
Fig. 2. Hα profile variations showing the development of the DACs. From bottom to top, JD 55 675, 55 688, 55 697, 55 703, and 55 712. Only the negative radial velocity components are shown, fluxes are scaled but the continuum is otherwise unnormalized.

The diffuse interstellar bands (DIBs), taken from the list by Friedman et al. (2011) for those most tightly correlated with extinction, provide an independent estimate of $E(B-V)$ for T Pyx. The equivalent widths are given in Table 3, the uncertainty being $\pm10\%$ for the measurements. Combining the extinction inferred from 5780, 6205, 6196, and 6283 Å gives $E(B-V) = 0.49\pm0.17$. The strongest DIBs, at 5780.5 Å and 6613.7 Å are shown in Fig. 1 along with the interstellar absorption lines listed in Table 2. The effect of this revision on the luminosity, in both quiescence and outburst is obvious, but the larger extinction also affects the derived properties of the WD based on the continuum from 1200–3000 Å (Selvelli et al. 2008). The increase in $E(B-V)$ in turn steepens the UV spectral gradient with wavelength such that the effective temperature of the WD is lower than earlier determinations (but we will discuss how much this change depends on a model atmosphere analysis in the next paper in this series).

4. Discrete absorption features

Our first observation, JD 55 667, was one day after the discovery and showed a fireball spectrum (see, e.g., Schwarz et al. 2001) dominated by P Cygni profiles of the H I Balmer lines
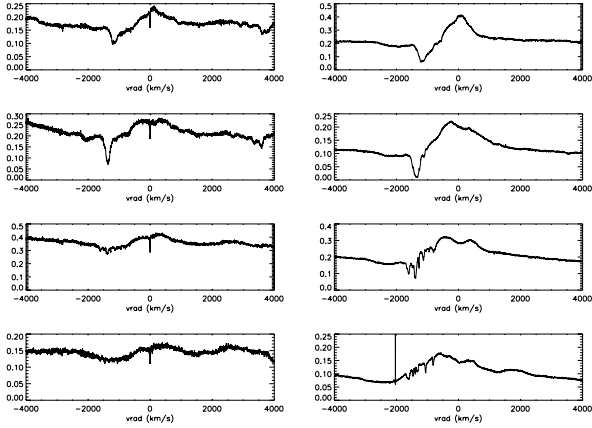
Fig. 3. Profile development for Fe II 4233.14 Å (RMT 26, *left*) and Fe II 5018.44 Å (RMT 42, *right*). *From top to bottom*, the dates are JD 55 688, 55 697, 55 703, and 55 712. In addition to the absorption components, note the change sin the emission near +2000 km s^{-1} (see text for discussion).

(Figs. 2 and B.1), He I, and and He II, for which the absorption extended without a terminal edge to ≈2500 km s^{-1}; Fig. 4 compares an example of the fireball stage profile of He I 5875 Å profile to the later appearing Na I D. The emission complex at 4640 Å due to C III and N III, was well-resolved into the two main contributors without an absorption trough being found on either. In subsequent spectra, we detected only low ionization Fe-peak transitions, Ca II H and K, and the Na I D doublet, all of which displayed increasingly complex sets of discrete high negative radial-velocity absorption components (DACs hereafter). The velocity components identified on the Fe II and Balmer lines on JD 55 703 are at –2964, –1661, –1543, –1433, –1303, –1153, –1056, –952, and –799 km s^{-1} with mean separations of Δv_{rad} = 122 ± 21 km s^{-1} and Δv ≤ 50 km s^{-1} for every component based on the Fe II RMT 42 lines[3]; the minimum width was ≈5 km s^{-1}. Subsequent velocity shifts are consistent with a linear velocity law for the ejecta. The broader *features* are likely blends of still optically thick individual components. If the velocity width relates directly to the filaments' linear thickness, then their filling factor may be quite low but their individual optical depths high (see below). The complexity of the radiative coupling between various levels of the iron group contributors to the atomic opacity is especially well illustrated by the behavior of three multiplets, Fe II RMT 27, 28, and 42. Of the first two, Fe II 4173.461, 4178.862, and 4233.167 showed a moving feature at –1200 km s^{-1} that displaced systematically toward higher velocity, that approximately coincided with the same feature in Fe II RMT 42 and the Balmer lines. These strong absorptions were short-lived. A third line in the multiplet, 5607.14 Å, showed nothing. In contrast, all three members of RMT 42 showed identical evolution (we display only 5018.44 Å, the strongest member of the triplet) and displayed persistent narrow lines even in the last observation. The lower level of RMT 26 and 27 is fed by transitions at 2500–2600 Å that, according to the Swift UVOT observations were becoming transparent by JD 55 703 (the analysis of the ultraviolet variations is postponed to a later paper). Examples of the line profiles for Fe II are shown in Fig. 3.

The fine structure that developed in the absorption lines was also mirrored in the emission component but with less complexity. This would be expected for a shell in expansion, the total

----

3 RMT refers to the *Revised Multiplet Tables*, Moore (1945).

----

optical depth, τ, decreasing with a similarity scaling with time t as $\tau \sim t^{-2}$ and individual features changing depending on the rates of ionization and recombination. In this interpretation, the fine structure was present from the earliest epoch, likely at the moment of ejection, but the visibility – contrast – of the features changed over time. The minimum velocity at which the fine structure absorption features appeared on the Fe II RMT42 lines was –572±5 km s^{-1} (JD 55 688). In the previous spectrum, these were blended within the broad absorption trough, whose minimum was at –635 km s^{-1}. However, the P Cyg features were separated from the emission (see Fig. 3) with a minimum at –270 km s^{-1}. The strongest line of the multiplet, 5169 Å, was the first to display the symmetric peaks and systematically displayed the strongest narrow absorption components. We note that the emission wing extended to the same maximum velocity as the absorption throughout this sequence. The Fe II lines on JD 55 712, are consistent with the development of a "thin shell" structure, with symmetric peaks at –376 and +476 km s^{-1}. The central velocity, v_{rad} = +60 km s^{-1}, is *consistent* with the detection of a high positive velocity component on the interstellar lines at >50 km s^{-1} and with a distance ≈5 kpc, if this velocity is the radial velocity of the T Pyx *system*. The emission peak shifted systematically from +20 km s^{-1} to +60 km s^{-1} before JD 55 712.

The Na I D lines, the only strong resonance transitions of a neutral species, are especially important when attempting to understand the profile variations. They showed the broad features but as the optical depth decreased, these too separated into an ensemble of narrow absorption components (see Fig. 4). The broad D1 feature, which shifted from –1900 to –2200 km s^{-1}, had no D2 counterpart. For every other (narrower) D1 component, there is a corresponding feature from D2. Chance coincidences, overlaps between a D1 feature with another from D2, account for their intensities, Discrete components as narrow as 10 km s^{-1} are detected and suggests that *all* of the broader features are, in fact, composite. Their individual optical depths decreased in time. As the outburst progressed, the emission component also broadened toward higher positive velocity with broad peaks that mirrored the absorption line velocities but with less distinct separation. This can be interpreted within the scenario of a ballistically expanding shell as the progression of a recombination front through the ejecta as the overall optical depth of the expanding ejecta decreased in time. If this is correct, the knots were present even in the earliest stage of the expansion but hidden by the more opaque overlying layers. The same effect was seen for the Fe II and H I Balmer lines but, arising from excited states, the interpretation is not so straightforward. The narrowest components, which agree in velocity and relative strength between the different ions, were only 10 km s^{-1} wide, indicating a low spatial filling factor but high individual column densities.

5. Discussion: the mass and structure of the ejecta

Perhaps the most significant result from these observations has been the insight they provide into the origin of the moving line systems observed in nova ejecta. It is unusual to have so long a plateau for a recurrent nova (although not for a classical nova) in the visible during which the UV is optically thick in lines from neutrals and singly ionized species. We do not know, at this point, *why* the ejecta from T Pyx are so massive. This episode is not unusual in terms of its rise, duration, or amplitude compared with previous outbursts and suggests that the ejection is not unusually massive relative to the historical events despite the long hiatus. Thus, the details provided by the NOT spectra
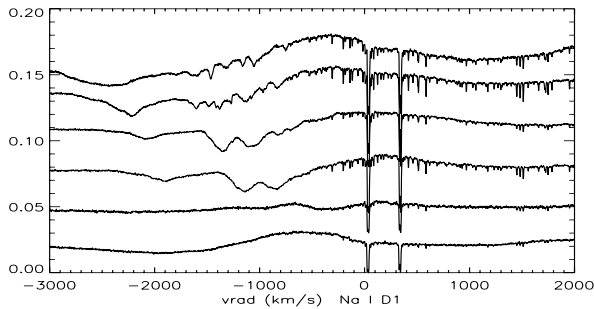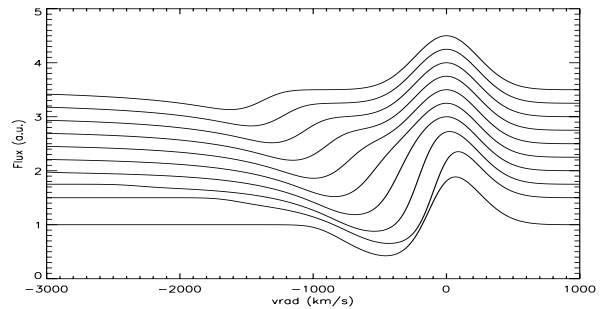
Fig. 4. The sequence of Na I D line variations for JD 55 667, 55 675, 55 688, 55 697, 55 703, and 55 712 (*from bottom to top*). Only He I 5875 Å is present in the first (JD 55 667, *bottom*) spectrum. The progressive displacement of the DACs, with the doublet. The spectrum from JD 55 690 is not included because of the lower signal-to-noise ratio (see text).
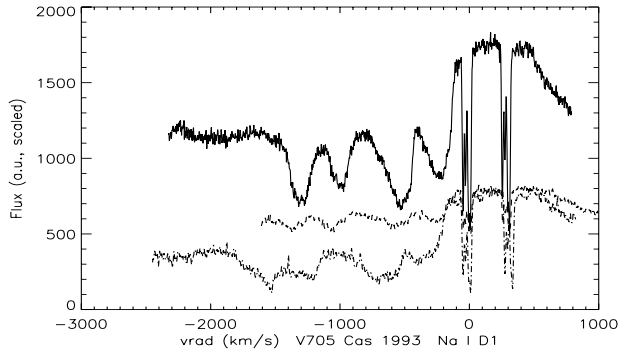

Fig. 5. Schematic model for the line variations, assuming a recombination front moving outward within separated ejecta that have individually a constant mass and linear velocity law. The emission-line profile is kept arbitrarily constant throughout the interval (see text).

are especially significant because they illustrate a *generic* behavior that is also seen in classical novae (Payne-Gaposchkin 1957; McLaughlin 1954, 1964).

The recombination of He II following the first observation, that occurred at an interval of about one week, provides an estimate of the electron density, $n_e \approx 2 \times 10^6$ cm^{-3} for the outer part of the ejecta at –2500 km s^{-1} at a radius of 1.5×10^{15} cm. Assuming a ballistic expansion with an r^{-3} radial dependence and an innermost shell velocity of 500 km s^{-1} based on the separation of the inner emission peaks on the Fe II profiles, the mass of a spherical, filled ejecta is $\approx 2 \times 10^{-5} f \, M_\odot$, where f is the radially constant filling factor. This is consistent with the long duration of the Fe-curtain phase, which lasted more than 50 days, and of the same order as the masses in classical novae for which such masses are normal but must be an upper limit. If, however, the shell were severely fragmented, as appears to be the case from the DACs, but every line of sight encountered at least one such optically thick filament, then the mass *could* be lower by a large factor. A filling factor $f \sim 0.01$ would reduce the mass estimate to that normally found for recurrent novae (e.g., Anupama 2008; Schaefer 2010) but requires that the individual filaments or substructures are extremely opaque and completely covering. This configuration is very difficult to achieve. A test is whether there is a constant bolometric luminosity phase similar to that found for classical novae (see e.g., Shore 2008), but that requires continued ultraviolet observations that have not yet been completed.

As a proof-of-concept, we show in Fig. 5 a schematic model for the absorption-line evolution that applies most simply to the Na I resonance lines (Fig. 4). This assumed a recombination front moving outward in the expanding ejecta. A constant velocity gradient with an r^{-3} density variation was imposed and the recombination was integrated through the ejecta. Each profile represents one time step, where the typical timescale is the recombination time from the disappearance of C III/N III 4640 Å and the He II lines between the first and second NOT observation, that is about 5 days. The intrinsic line profile was assumed to be Gaussian, but the details are not important for this simulation. The decrease in the total optical depth, scaling as t^{-2}, and the separation of the absorption component have been reproduced. The individual fine structure features were not included, they would be part of the absorption in any velocity interval, nor is the emission (only an invariant Gaussian was used to render the absorption visible because the ejecta are assumed to be detached from the white dwarf). The line evolution can thus be understood by assuming only that the structure was frozen in the ejecta at the time of expulsion. There is no need for either colliding shocks and winds (Kato & Hachisu 2007) or subsequent collisions with circum-system material (e.g., Williams et al. 2008; Williams & Mason 2010), although the latter may also occur. The evolution of the different DACs can be explained by the changes in the optical depth of specific transitions in the ultraviolet as the ejecta expand. Finally, the last NOT spectrum shows weak emission appearing on [O I] 5577 and 6300 Å with a double-peaked structure that is consistent with with the innermost part of the ejecta becoming optically thin in the ultraviolet and beginning to again display both He I and [O I] emission lines.

References

Anupama, G. C. 2008, in RS Ophiuchi (2006) and the Recurrent Nova Phenomenon, ed. A. Evans, M. F. Bode, T. J. O'Brien, & M. J. Darnley (San Francisco: ASP), ASP Conf. Ser., 401, 31
Bode, M., & Evans, A. 2008, The Classical Novae, 2nd ed. (Cambridge: Cambridge Univ. Press)
Brand, J., & Blitz, L. 1993, A&A, 275, 67
Friedman, S. D., York, D. G., McCall, B. J., et al. 2011, ApJ, 727, 33
Kalberla, P. M. W., Burton, W. B., Hartmann, D., et al. 2005, A&A, 440, 775
Kato, M., & Hachisu, I. 2007, ApJ, 657, 1004
McLaughlin, D. B. 1954, ApJ, 119, 124
McLaughlin, D. B. 1964, AnAp, 27, 405
Moore, C. E. 1945, CoPri, 20, 1
Payne-Gaposchkin, C. 1957, The Galactic Novae (Amsterdam: North-Holland)
Sadakane, K.,Tajitsu, A., Mizoguchi, S., et al. 2010, PASJ, 62, L5
Schaefer, B. 2010, ApJS, 187, 275
Schlegel, D. J., Finkbeiner, D. P., & Davis, M. 1998, ApJ, 500, 525
Schwarz, G. J., Shore, S. N., Starrfield, S., et al. 2001, MNRAS, 320, 103
Selvelli, P., Cassatella, A., Gilmozzi, R., & Gonzez-Riestra, R. 2008, A&A, 492, 787
Shore, S. N. 2008, in The Classical Novae ed. M. F. Bode, & A. N. Evans, 2nd ed. (Cambridge: Cambridge Univ. Press)
Starrfield, S., Sparks, W. M., & Truran, J. W. 1985, ApJ, 291, 136
Starrfield, S., Iliadis, C., & Hix, R. W. 2008, in The Classical Novae, ed. M. F. Bode, & A. N. Evans, 2nd ed. (Cambridge: Cambridge Univ. Press)
Uthas, H., Knigge, C., & Steeghs, D. 2010, MNRAS, 409, 237
Williams, R., & Mason, E. 2010, Ap&SS, 327, 207
Williams, R., Mason, E., Della Valle, M., & Ederoclite, A. 2008, ApJ, 685, 451

Page 5 is available in the electronic edition of the journal at `http://www.aanda.org`

Fig. A.1. V705 Cas (Ritter Observatory spectra of the optically thick stage of the CO nova Nova Cas 1993, Na I D line variations. *Top*: 1993 Dec. 27. *Middle*: 1993 Dec. 29, 1994. *Bottom*: 1994 Jan. 5 (see text for details)

Appendix A: V705 Cyg 1993 and discrete absorption systems on Na I D

The D lines have been found to display P Cyg profiles occasionally in the literature, notably during the first phase of the DQ Her 1934 outburst (see McLaughlin 1954, 1964). However, based on photographic, uncalibrated, and relatively low resolution spectra, this might be explained as variations in the complex of emission and absorption lines normally seen in the initial stage of the expansion. The first classical CO nova to show this phenomenon unambiguously after the advent of CCD detectors, V705 Cas 1993, is shown in Fig. A.1. This sequence shows the optically thick phase, during the first two weeks of the outburst. The line pairs shifted systematically to higher velocity with an increasing optical depth, indicated by the increase in the $F(5895)/F(5889)$ ratio, with $FWHM \approx 300$ km s^{-1}. The sequence ended quite early in the outburst, the nova forming dust about two months later (Shore et al. 1994), as did DQ Her and several other novae in which the Na I D multiple components and moving DACs were historically observed. The NOT sequence for T Pyx covered a longer interval. Similar behavior has recently been detailed by Sadakane et al. (2010) for V1280 Sco.

Appendix B: Additional figure
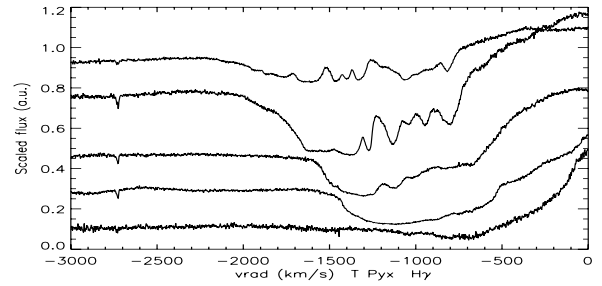
Fig. B.1. Hγ profile variations, as in Fig. 2.